

Electromagnetic tracking in guided medical interventions

Herman Alexander Jaeger, Kilian O'Donoghue, and Pádraig Cantillon-Murphy
Tyndall National Institute, Cork, Ireland

Abstract

Electromagnetic tracking is a navigation technology used in guided medical interventions. The technology is gaining popularity in the fields of robotic surgery, catheter navigation and human-machine interface design. Small magnetic sensors provide enable the position and orientation of a surgical instrument to be tracked in real-time without line of sight. This paper discusses how low frequency electromagnetic fields are used as a tracking medium to precisely estimate the pose of magnetic sensors. The quasi-static approach to magnetic field modelling is presented along with number of pose estimation methods. Advantages and disadvantages of each system type are also discussed.

1 Introduction

Electromagnetic tracking is seeing significant uptake in guided medical procedures and increased integration within new surgical instruments. Commercially available magnetic tracking systems include the NDI Aurora and Trakstar (Northern Digital, Waterloo, Canada) which are widely used in the medical device industry. Other OEM electromagnetic tracking system manufacturers include Polhemus (Vermont, USA) and AmfiTeck (Vejlø, Denmark). Many large medical device companies implement their own proprietary in-house electromagnetic tracking solutions that are specific to a single clinical application.

Novel applications of electromagnetic tracking technology are frequently published and aim improve the safety and efficiency of medical procedures. Some highlights include the development of a dental implant guidance system [1], wireless gastrointestinal endoscopy capsule tracking [2], orthopaedic intra-medullary nail placement [3, 4], guided bronchoscopy [5] and electrophysiology mapping [6].

Electromagnetic tracking systems operate by sensing the magnetic field at a point in space. Tracking systems can use either solid-state or passive sensor technology, however the majority of commercially available tracking systems use passive inductive coil sensors due to their low hazard risk, high magnetic sensitivity and ease of integration within medical devices. Fig. 1 shows the design of an example electromagnetic tracking system. A transmitter creates a magnetic excitation field \mathbf{B} and is powered by a control unit.

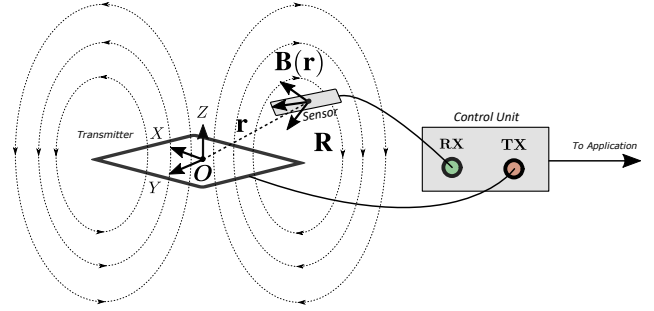


Figure 1. An electromagnetic tracking system.

A magnetic sensor is also connected to the control unit which detects a signal at a location \mathbf{r} and orientation \mathbf{R} within the excitation field. Resolving the sensor's position and orientation, also known as the pose, is generally performed by comparing a magnetic model of system with received sensor measurements. The system topology determines whether a solution to the pose problem can be obtained analytically, or whether a numerical solver must be used. Tracking systems can resolve either a five or six degree-of-freedom (6-DoF) poses depending on the design of the sensor. A classic 6-DoF system design is shown in Fig. 2. The Cartesian position of the sensor relative to the system origin O is represented by the vector \mathbf{r} given by

$$\mathbf{r} = (x, y, z) \quad (1)$$

and the orientation of the sensor \mathbf{R} is given by

$$\mathbf{R} = (\theta, \varphi, \gamma) \quad (2)$$

where x , y and z are Cartesian position coordinates and θ , φ and γ are the elevation, azimuth and the roll angles of the sensor relative to the system origin, in radians.

2 Tracking system types

The first electromagnetic tracking systems utilised a triaxial coil source with magnetic moments ($\mathbf{M}_1, \mathbf{M}_2, \mathbf{M}_3$) and an orthogonal triaxial sensor array to form an orthogonal transmit-receive pair shown in Fig. 2 [7]. The resulting pose estimation problem contains six degrees of freedom, however the orthogonal nature of the system allows for mutual independence of the solutions for the position and orientation respectively. A single measurement from a triaxial

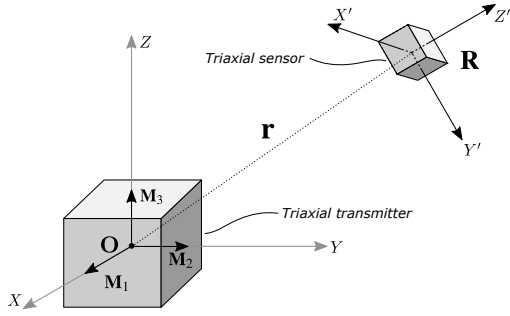


Figure 2. Triaxial tracking system described in [7].

sensor is therefore sufficient to provide a unique analytical solutions for the pose in which position and orientation resolved in separate calculations. In fact, only two transmitter coils are required to determine the position of a three axis sensor, provided some additional calculations are performed to resolve ambiguities [8]. This tracking method allows for fast and deterministic tracking performance suitable for real-time computation and can be performed on relatively low-powered hardware.

An alternative approach to magnetic tracking uses a set of non-orthogonal transmitter coils with magnetic moments ($\mathbf{M}_1 \dots \mathbf{M}_N$) and a single-axis sensor as shown in Fig. 3. Single-axis sensors are preferable in medical devices since they can be manufactured into narrow solenoids as shown in Fig. 4 which makes them ideal for embedding within medical instruments. However, such a design increases the mathematical complexity of the pose estimation problem since the sensor is limited to detecting the magnetic field along one axis instead of three. The solutions for the position and orientation are no longer independent of one another and are instead tightly coupled. In addition, the solenoidal shape of the sensor introduces a rotational ambiguity about its axis, thus making γ indeterminate. The resulting pose estimation problem therefore contains five degrees of freedom whose variables must all be solved simultaneously. Solutions are generally implemented by a minimising cost functions of the form

$$\underset{\mathbf{r}}{\text{minimize}} \sum_{i=1}^N (V_i - K_i \Phi_i(\mathbf{r})) \quad (3)$$

where N is the total number of transmitting coils, V_i is the received sensor signal from the i^{th} transmitter coil, Φ_i is the modelled magnetic flux contribution at the pose \mathbf{r} from the i^{th} coil, and K_i is a scalar obtained through calibration [9, 10]. Obtaining a solution requires the use of non-linear solvers. Iterative solvers such as trust region and Levenberg-Marquardt algorithms [11, 12] are non-deterministic in terms of the time required to achieve convergence, since they depend on many parameters including the shape of the cost function at the global minimum as well as user-defined termination settings. Systems of this type generally require eight or more transmitter coils in order to obtain reliable data at all sensor poses and prevent zones of unreliable tracking due to low-resolution field regions [13].

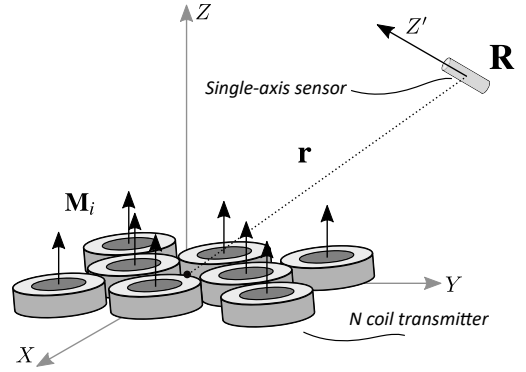


Figure 3. Single axis sensor tracking system.

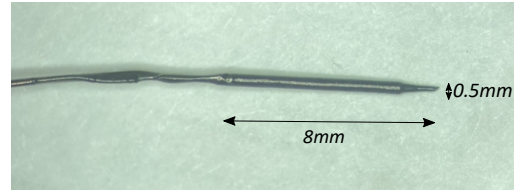


Figure 4. 5-DoF single axis sensor.

3 Quasi-static magnetic models

The electromagnetic field produced by oscillating charge in an antenna consists of three distinct regions: the near-field, the far-field and a transition region between the two called the Fresnel zone. The near-field, also called the reactive field, exists in the space near the antenna. The size of region depends on the wavelength, λ , of the excitation signal as can be approximated as being within $(\lambda/2\pi)$ meters of an antenna structure [14]. In this region the electromagnetic field is dominated by electric and magnetic field components that are decoupled from one another. Electromagnetic tracking systems operate with excitation frequencies between 1 kHz and 20 kHz corresponding to wavelengths between 300 m and 15 m. The working volume of electromagnetic tracking systems is on the order of 1 m to 1.5 m, meaning that these systems can generally be treated as operating entirely within the near-field. Propagation of electromagnetic waves can be ignored in this instance, provided that the excitation frequencies remain sufficiently low.

Using low-frequency excitation signals brings substantial design benefits in terms of magnetic field modelling. The excitation signal wavelengths of interest are orders of magnitude larger than the working dimensions of the tracking system hence a quasi-static modelling approach can be taken for determining the transmitter's magnetic field distribution. We can apply Maxwell's equations for magnetostatics

$$\oint \mathbf{B} \cdot d\mathbf{A} = 0 \quad (4)$$

$$\oint \mathbf{B} \cdot d\mathbf{L} = \mu_0 I \quad (5)$$

since the current density is assumed uniform at any moment in time for the low-frequency excitation signals being con-

sidered. These static conditions allow expressions for the magnetic field to be developed in a simple manner, provided the geometry of current is known. Contrary to a purely magnetostatic system, Faraday's law may be reintroduced to predict the changing magnetic flux once the static magnetic field distribution is known. The induced induced sensor emf ε due to the transmitter field can therefore be expressed as

$$\varepsilon = \frac{d\Phi}{dt} \quad (6)$$

where Φ is the magnetic flux cutting the axis of a magnetic induction sensor given by

$$\Phi = \int \mathbf{B}(\mathbf{r}) \cdot d\mathbf{A}_s \quad (7)$$

where $\mathbf{B}(\mathbf{r})$ is the magnetostatic flux density at a point \mathbf{r} , and \mathbf{A}_s is the cross sectional area of the sensor. A number of different formulations are used to evaluate the magnetic flux density $\mathbf{B}(\mathbf{r})$ which depend on the geometry of the transmitter coils and will be discussed next.

A widely adopted approach for modelling magnetic field of a transmitter is by approximating each magnetic source with that of a dipole [10]. The expression for the field produced by a magnetic source can be described as a dipole if the region of interest for magnetic measurements is significantly greater than the largest dimension of the source [14]. Assuming this assumption holds then near-field magnetic field of a source can be described as

$$\mathbf{B}(\mathbf{r}) = \frac{\mu_0}{4\pi} \left(\frac{3(\mathbf{M} \cdot \mathbf{r})\mathbf{r}}{r^5} - \frac{\mathbf{M}}{r^3} \right) \quad (8)$$

where \mathbf{M} is the equivalent magnetic dipole moment of the source and \mathbf{r} is the location at which the field is evaluated. The dipole model as therefore very simple and requires little computational overhead. A drawback of such a model is that sensors must maintain a minimum distance from the magnetic sources, otherwise the dipole model approximation becomes invalid and introduces tracking errors. Systems using this modelling method therefore typically use small circular coils as magnetic sources [15].

If the mechanical dimensions of the transmitter coils are of the same order as the tracking volume then the magnetic dipole approach will result in erroneous pose estimation data. In this case a more complicated model must be used to evaluate the magnetic flux density as a function of space. Assuming a thin wire, the magnetic field at any point in space can be computed using the Biot-Savart law:

$$\mathbf{B}(\mathbf{r}) = \frac{\mu_0}{4\pi} \int_C \frac{I d\mathbf{L} \times \mathbf{r}'}{|\mathbf{r}'|^3} \quad (9)$$

where I is the current flowing in wire loop and $d\mathbf{L}$ is a differential segment of the wire geometry, and \mathbf{r}' is the displacement vector pointing from $d\mathbf{L}$ to the location at which

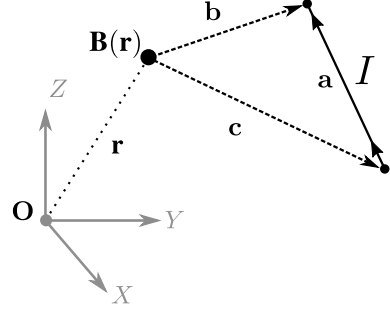


Figure 5. Vectors shown in (10)

the field is computed. Integrating this expression over a wire large circular loop yields expressions for the magnetic field which contains complete elliptic integrals of the first and second kind [16, 17]. For brevity the expressions have been omitted here but are described in detail in the references. The resulting field expressions are not trivial to calculate and require substantial computation compared to the dipole method. An advantage of this approach is that the field description is no longer an approximation thus allowing magnetic sensors to be tracked much closer to the magnetic source.

A compromise between between the dipole approximation and the full loop coil models is to use a current filament approach [9]. Optimisations to the integral in (9) can be performed depending on the geometry of the magnetic transmitter coils. If one assumes a coil consisting solely of straight and finite current filaments then the expression for the magnetic field of a single filament can be simplified to

$$\mathbf{B}(\mathbf{r}) = \frac{\mu_0 I}{4\pi} \left(\frac{\mathbf{c} \times \mathbf{a}}{|\mathbf{c} \times \mathbf{a}|^2} \right) \left(\frac{\mathbf{a} \cdot \mathbf{c}}{|\mathbf{c}|} - \frac{\mathbf{a} \cdot \mathbf{b}}{|\mathbf{b}|} \right) \quad (10)$$

where \mathbf{a} is a vector representing the length and direction of a current carrying conductive filament. The vector \mathbf{r} points to the observation point from which the field is measured. Vectors \mathbf{c} and \mathbf{b} point from the observer position \mathbf{r} to the start and end points of the current filament respectively [18]. These vectors are shown in Fig. 5. It is interesting to note that this closed-form expression consists entirely of finite linear operations. The calculation for the total magnetic field produced by a multi-turn coil as shown in Fig. 6 must consider the field produced by each individual current filament. Summing the individual field contributions yields

$$\mathbf{B} = \sum_{i=1}^{k-1} \mathbf{B}_i(\mathbf{r}) \quad (11)$$

where $k - 1$ is the total number of current filaments comprising a coil defined by k points. Computation of the magnetic fields in this manner can be parallelised with appropriate hardware since each contribution is unique and independent. Coils of this type can be easily manufactured using printed-circuit board technology, in which case the length of each current filament, \mathbf{a} , is derived from the board geometry [9].

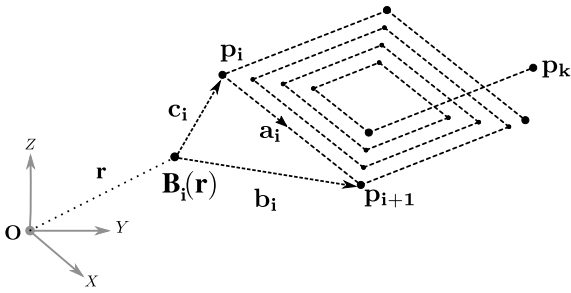


Figure 6. A square coil consisting of multiple filaments.

4 Conclusion

Electromagnetic tracking is a core technology in guided surgery with applications including bronchoscopy, electrophysiology, dentistry and orthopaedics. A number of magnetic tracking and modelling approaches were discussed with references provided to key papers.

References

- [1] Y. Gao, C. Qin, B. Tao, J. Hu, Y. Wu, and X. Chen, "An electromagnetic tracking implantation navigation system in dentistry with virtual calibration," *The International Journal of Medical Robotics and Computer Assisted Surgery*, vol. 17, no. 2, p. e2215, 2021.
- [2] S. Song, S. Wang, S. Yuan, J. Wang, W. Liu, and M. Q.-H. Meng, "Magnetic Tracking of Wireless Capsule Endoscope in Mobile Setup Based on Differential Signals," *IEEE Transactions on Instrumentation and Measurement*, vol. 70, pp. 1–8, 2021.
- [3] P. Tu, Y. Gao, A. J. Lungu, D. Li, H. Wang, and X. Chen, "Augmented reality based navigation for distal interlocking of intramedullary nails utilizing Microsoft HoloLens 2," *Computers in Biology and Medicine*, vol. 133, p. 104402, Jun. 2021.
- [4] S. Sharma, A. Telikicherla, G. Ding, F. Aghlmand, A. H. Talkhooncheh, M. G. Shapiro, and A. Emami, "Wireless 3D Surgical Navigation and Tracking System with 100 micron Accuracy Using Magnetic-Field Gradient-Based Localization," *IEEE Transactions on Medical Imaging*, pp. 1–1, 2021.
- [5] T. Ishiwata, H. Ujiie, A. Gregor, T. Inage, Y. Motooka, T. Kinoshita, M. Aragaki, Z. Chen, A. Effat, N. Bernards, and K. Yasufuku, "Pilot study using virtual 4-D tracking electromagnetic navigation bronchoscopy in the diagnosis of pulmonary nodules: a single center prospective study," *Journal of Thoracic Disease*, vol. 13, no. 5, pp. 2885–2895, May 2021.
- [6] T. Skála and M. Táborský, "Electromechanical mapping in electrophysiology and beyond," *Cor et Vasa*, vol. 57, no. 6, pp. e470–e482, Dec. 2015.
- [7] F. H. Raab, E. B. Blood, T. O. Steiner, and H. R. Jones, "Magnetic Position and Orientation Tracking System," *IEEE Trans. Aerosp. Electron. Syst.*, vol. 5, no. 5, pp. 709–718, 1979.
- [8] F. H. Raab, "Quasi-Static Magnetic-Field Technique for Determining Position And Orientation," *IEEE Transactions on Geoscience and Remote Sensing*, vol. GE-19, no. 4, pp. 235–243, Oct. 1981.
- [9] K. O'Donoghue, D. Eustace, J. Griffiths, M. O'Shea, T. Power, H. Mansfield, and P. Cantillon-Murphy, "Catheter position tracking system using planar magnets and closed loop current control," *IEEE Transactions on Magnetics*, vol. 50, no. 7, pp. 1–9, 2014.
- [10] A. Plotkin, V. Kucher, Y. Horen, and E. Paperno, "A new calibration procedure for magnetic tracking systems," *IEEE Transactions on Magnetics*, vol. 44, no. 11, pp. 4525–4528, 2008.
- [11] R. Byrd, R. Schnabel, and G. Shultz, "A Trust Region Algorithm for Nonlinearly Constrained Optimization," *SIAM Journal on Numerical Analysis*, vol. 24, no. 5, pp. 1152–1170, 1987, publisher: Society for Industrial and Applied Mathematics.
- [12] K. Levenberg, "A Method for the Solution of Certain Non-Linear Problems in Least Squares," *Quarterly of Applied Mathematics*, vol. 2, pp. 164–168, 1944.
- [13] E. Paperno and P. Keisar, "Three-dimensional magnetic tracking of biaxial sensors," *IEEE Transactions on Magnetics*, vol. 40, no. 3, pp. 1530–1536, 2004.
- [14] D. K. Cheng, *Field and Wave Electromagnetics*, 2nd ed. Addison-Wesley, 1989.
- [15] A. Plotkin and E. Paperno, "3-D Magnetic Tracking of a Single Subminiature Coil with a Large 2-D Array of Uniaxial Transmitters," *IEEE Transactions on Magnetics*, vol. 39, no. 5, pp. 3295–3297, 2003.
- [16] A. Plotkin, O. Shafrir, E. Paperno, and D. M. Kaplan, "Magnetic eye tracking: A new approach employing a planar transmitter," *IEEE Transactions on Biomedical Engineering*, vol. 57, no. 5, pp. 1209–1215, 2010.
- [17] A. Plotkin, E. Paperno, G. Vasserman, and R. Segev, "Magnetic tracking of eye motion in small, fast-moving animals," *IEEE Transactions on Magnetics*, vol. 44, no. 11, pp. 4492–4495, 2008.
- [18] C. L. W. Sonntag, M. Sprée, E. A. Lomonova, J. L. Duarte, and A. J. A. Vandenput, "Accurate Magnetic Field Intensity Calculations for Contactless Energy Transfer Coils," in *Proceedings of the 16th International Conference on the Computation of Electromagnetic Fields, Aachen, Germany, Aachen, Germany, 2007*, pp. 1–4.